Near-infrared Raman instrument for rapid and quantitative measurements of clinically important analytes

Jianan Y. Qu[a] and Lan Shao
Department of Electrical and Electronic Engineering, Hong Kong University of Science and Technology, Clear Water Bay, Kowloon, Hong Kong, People's Republic of China

(Received 3 January 2001; accepted for publication 18 March 2001)

We present the use of a near-infrared (IR) laser Raman spectroscopy instrument to measure the concentrations of many important analytes at their clinically relevant levels in the simulated human serum. The Raman signal is generated by a 745 nm diode laser in a disposable waveguide capillary cell that contains a submicroliter sample. The Raman spectrum is acquired from the sample in 10 s. The major error in quantitative Raman spectroscopy caused by the variation in laser power, optical alignment, and capillary cell size from measurement to measurement is eliminated by normalizing the spectrum to the dominant water peak at 3350 cm^{-1}. Concentrations of glucose, acetaminophen, albumin, and other analytes are predicted using partial least squares (PLS) calibration. An effective multiple bandpass-filtering method was developed to enhance the signal of the desired analytes to interfering background ratio for improvement of PLS calibration accuracy. It is demonstrated that the accuracy of predicted concentrations for all analytes in the simulated human serum samples are highly acceptable for clinical diagnosis. The results promise the potential applications of the near-IR Raman instrument in medical practice. © *2001 American Institute of Physics.*
[DOI: 10.1063/1.1372170]

I. INTRODUCTION

Raman spectroscopy measures the vibrational frequencies of molecules that are related to the molecular structures. The Raman spectra provide both the unique fingerprints and quantitative information of the molecules present in a sample under examination. The Raman spectroscopic method can therefore identify and quantify multiple analytes simultaneously without using a reagent. When compared with conventional reagent-based analytical techniques, the Raman technique offers the advantages of rapidness of measurement, low operation cost over the long run and, in particular, the screening of the analytes of interest in a multicomponent mixture. In principle, infrared (IR) absorption spectroscopy, a competing optical technique, can perform the same measurements as the Raman method. However, for aqueous solutions, the IR absorption spectra of the desired molecules fall within the dominant water absorption or overtone bands that create large background and introduce interference to the measurements. In contrast, the Raman spectrum of water has a simple structure and consists of relatively narrow peaks that can be separated from the Raman spectra of other molecules.

Although Raman spectroscopy offers the significant advantage of being a reagentless analytical method, its application to biomedical problems is relatively new. Over the past 10 years, Raman spectroscopy has gained increasing prominence as a quantitative tool for the analysis of biological samples because of technological advances in engineering the excitation source (diode laser) and the detection device [cooled deep depletion charge coupled device (CCD)]. Raman measurements of metabolites and therapeutic drugs were performed in solutions of water or single solvents.[1–5] Very recently, researchers from the Massachusetts Institute of Technology and our group demonstrated that Raman spectroscopy can measure important metabolites at their physiological levels in human sera.[6,7] The measurement accuracy was clinically acceptable. However, there are a few obstacles that make conventional Raman systems impractical in clinical practice. First, since Raman scattering is inherently weak, the signal acquisition time must be long enough (1–5 min) to obtain the Raman spectra of serum samples with decent signal-to-noise ratio (SNR),[6,7] though the detectors were cooled using liquid nitrogen. Second, the signals of many desired analytes at their clinically relevant levels are much smaller than the signals of background substances such as proteins. Sample preprocessing is needed to remove the interfering large molecules and to improve the measurement accuracy of molecules with relatively small Raman signals.[6] Moreover, the quantitative measurement requires an absolutely reproducible geometry of excitation light delivery and Raman signal collection and precise monitoring of laser power.

This study aims to overcome the problems discussed earlier. We used a waveguide capillary as the Raman cell that requires less than 1 μl sample for the measurement. The compact optical fiber arrays was used to collect the Raman signal with high efficiency. To record the signal with a good SNR, an acquisition time as short as 10 s was achieved. For each measurement, the Raman spectrum was normalized to the dominant water peak at 3350 cm^{-1}. This self-calibration method eased the restrictive requirements for the reproduc-

[a]Author to whom correspondence should be addressed; electronic mail: eequ@ust.hk

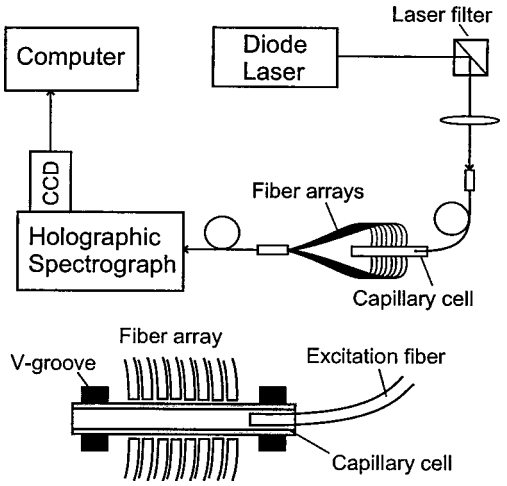

FIG. 1. Schematic of the near-IR laser Raman instrument.

ibility of excitation/collection geometry and the precisely monitoring of laser power. Finally, we developed a multiple bandpass-filtering technique to increase the signal of the desired analyte to the interfering background ratio. The accuracy of the predicted concentrations of the desired analytes in the sample is substantially improved by coupling the digital filtering techniques and the multivariate calibration method.

II. INSTRUMENTATION

The schematic of the near-IR laser Raman instrument is shown in Fig. 1. The excitation source was a diode laser (model PI-ECL-745-300, Process Instruments, Inc.) with a wavelength of 745 nm and output of 150 mW. The amplified spontaneous emission of the laser was removed with a holographic filter. The filtered beam was then focused into a 100 μm fiber that conducted the excitation light to a capillary Raman cell. The cell became a waveguide when it was filled with the sample. The excitation light was completely guided in the cell and generates a line source of Raman signals as it propagated along the capillary. The waveguide cell was first introduced by Walrafen and Stone in 1972[8] and has been widely used in Raman, absorption and fluorescence spectroscopy since then. A detailed schematic of the Raman cell and collection fiber optics is also shown in Fig. 1. The Raman cell was a homemade disposable quartz capillary with an inner diameter ranging from 250 to 300 μm and a length of 20 mm. The sample was drawn into the cell by capillary force. The optical fiber conducting the excitation light was inserted into the cell. The cell position was secured with a pair of V-groove holders. The Raman cell was disposed after each measurement.

Since the spontaneous Raman signal emits to a 4π solid angle, a large portion of the Raman emission was unguided by the capillary waveguide and was collected from the side of the cell. The arrangement of signal collection in this work was similar to the side-view type of waveguide cells reported in Ref. 9. To make the instrument compact, we used two optical fiber arrays instead of imaging optics to collect the Raman signal as shown in Fig. 1. Each fiber array consisted of eight single fibers each with a diameter of 350 μm. The distance between the distal tips of the arrays and the capillary surface was about 200 μm. The other ends of the arrays were combined together and lined up to form a 0.35×6 mm entrance slit for a single-stage holographic grating imaging spectrograph (model No. HoloSpec f/1.8i, Kaiser Optical Systems, Inc.). The numerical aperture of the fiber array was matched with that of the spectrograph. A liquid nitrogen cooled two-dimensional CCD (model LN/CCD-1340/400-EB/1, RS Roper Scientific) was used to record the Raman spectra. The Raman signals from the fibers were dispersed by the spectrograph with wave number resolution of 20 cm^{-1}. Raman spectra were formed by binning over 400 pixels of the CCD vertically.

III. EXPERIMENTAL METHOD

A. Samples

The simulated serum samples were made with mixtures of glucose, urea, triactin, albumin, globulin, acetaminophen, and ethanol in phosphate-buffer saline (PBS). The triactin was used to model the triglyceride.[10] Glucose, urea, triglyceride, albumin, and globulin are major metabolites in human serum. Acetaminophen and ethanol are, respectively, the commonly tested overdosed therapeutic drug and substance of abuse in clinical chemistry laboratories. They become toxic when their concentrations in blood are over certain levels. We added them into the simulated sera to test the ability of the Raman instrument in the screening of toxic substances in blood sample.

Three sets of samples were prepared for different purposes. The first set included five aqueous stock solutions of pure glucose, urea, triactin, ethanol, and acetaminophen. We used them to extract the pure Raman spectra of the five analytes. To ensure the extraction of the pure spectrum with a high SNR for the development of multiple bandpass filters, concentrations of glucose, urea, triactin, ethanol, and acetaminophen were set to 30 and 30 mM, 5 g/l, 100, and 30 mM, respectively. These levels were a few times higher than their mean physiological levels and toxic levels.[11,12] The second set of samples was prepared with 30 mixtures of glucose, urea, triactin, ethanol, and acetaminophen in PBS. The third set of samples consisted of 30 mixtures of all the five analytes and representative proteins (albumin and globulin) in PBS. The two sets of samples were used to simulate the sera with and without protein molecules removed by sample preprocessing procedures, respectively.[7] The metabolites in the second and third sets of samples were present in the levels spanning the physiological ranges of humans.[11] The concentration ranges of ethanol and acetaminophen covered their toxic levels in human blood.[12] Specifically, glucose, urea, triactin, ethanol, and acetaminophen in the second set of samples were prepared at 30 different levels spanning the range 1–11, 2–10 mM, 0.5–5 g/l, 0–46, and 0–10 mM, respectively. The concentrations of the five individual analytes were randomized in each sample to eliminate a possible correlation in the samples. In the third set of samples, the concentrations of albumin and globulin were in the ranges 27–64 and 20–40 g/l, respectively. The concentrations of other five analytes were in the same ranges as in the second set of samples. Again, the concentrations of all the analytes

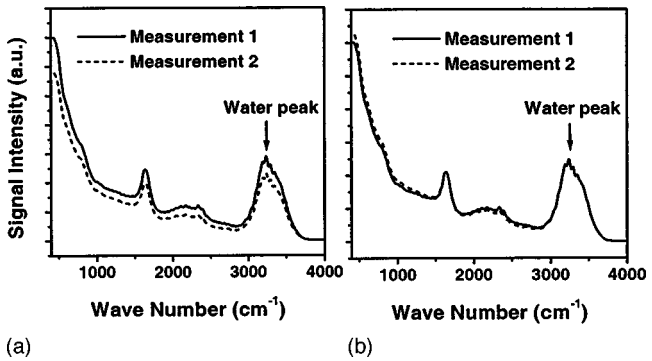

FIG. 2. Raman spectra of water. (a) Raw signals. (b) Normalized signals.

in each sample were randomly set. All the analytes used in preparation of the three sets of samples were reagent grade and purchased from Sigma Chemical Co. (St. Louis, MO).

B. Raman signals

For the measurement of each sample, the power of the laser was retained at 100 mW. It was found that the 10 s acquisition time was adequate to record the spectral data with decent SNRs, compared with the few minutes of acquisition time required by other Raman systems.[6,7] To observe the possible thermal degradation of the sample caused by the guided laser in the capillary, we repeated the Raman measurements with an acquisition time of 60 s for five times on two samples randomly picked from the second and third sets. Comparison of the five spectra recorded consecutively from each sample indicates that no obvious change was observed. This means that the possible thermal degradation of samples caused by excitation laser was negligible.

In quantitative Raman spectroscopy, a general problem is that the excitation/collection geometry and excitation power may vary from measurement to measurement. This introduces errors into Raman quantification because the signal is related to the excitation/collection optics and is linearly proportional to the excitation power. It is known that water is the dominant solvent in serum. The Raman spectrum of water has a strong peak at 3350 cm^{-1}. We took the water peak as the reference and normalized the entire Raman spectrum to it. In this way, the Raman signal can be self-calibrated. We demonstrate the calibration of Raman signal in Fig. 2. The pure water signals shown in Fig. 2(a) were recorded from two measurements with the Raman cells of almost the identical size. The difference in signal intensity between the two measurements is obvious because of the irreproducible alignment, though the measured sample was the same. After normalizing the signal to the water peak at 3350 cm^{-1}, the results of two measurements shown in Fig. 2(b) became almost identical and the errors caused by the factors discussed earlier were removed.

C. Calibration and digital filtering

The Raman spectra of all analytes in a sample are excited simultaneously and overlap each other. It is impossible to measure an analyte through a straightforward peak analysis. The multivariate calibration techniques are frequently used to identify and quantify analytes of interest in a multicomponent mixture. The partial least square regression (PLS) has been proved as one of the most effective multivariate calibration techniques.[13] In PLS calibration, the model for concentration prediction is built on the calibration set, which is a series of spectral data collected from samples of known chemical profiles.[14,15] However, confounding of the desired signal with interferants, such as irrelevant components, noise and baseline variation, will affect the accuracy of the PLS prediction. In particular, the calibration model can be severely corrupted when the desired signal is much smaller than that of interferants in a multicomponent mixture. For instance, we found that the glucose signal at the necessary physiological level in human serum is hundreds of times weaker than the protein signals.[7] The PLS calibration model built on the Raman spectral data from human serum samples was a poor predictor of glucose concentration. To demonstrate that the large molecules were the major interferants causing the PLS prediction error, we removed them by ultrafiltration. The prediction accuracy of glucose concentration was then found to be tremendously improved.[7] Though the ultrafiltration can ''physically'' eliminate the major interference, it introduces an additional technical complexity for the Raman tests. An approach that does not require complicated preprocessing of samples and that can improve the multivariate calibration is therefore more desirable.

Various methods, such as digital filtering,[10,16] wavelet analysis,[17] and variable selection techniques,[18–21] have been studied to reduce the prediction error in PLS caused by uninformative signals that confound the calibration model. It has been demonstrated that better results could be obtained by preprocessing the raw spectral data with the methods to remove artifacts prior to the building of the calibration model. It should be noted that all the existing methods do not use the pure spectrum of the desired analyte as known *a priori* in the procedures of spectral preprocessing. Recently, a linear multivariate calibration method, called hybrid linear analysis, was reported.[22] It incorporates the spectrum of the analyte of interest into the calibration and achieves better prediction accuracy than PLS. Here, we propose a digital filtering method that is used to process the raw spectral data and to enhance the signal of desired analyte-to-interference background ratio (SBR) before applying the PLS calibration. The filter is built by taking advantage of knowing both the pure spectrum of the desired analyte and spectra of biological analyte mixtures in the calibration set. The development of this filtering technique was motivated by the work reported in Refs. 10, 16, and 22.

In the case that the signal of the desired analyte, $p(k)$, is much smaller than that of the multicomponent mixture, $s(k)$, the interfering background can be well approximated well by $s(k)$. Mathematically, an optimization problem can be formulated to maximize the SBR after the filtering is applied to the calibration spectral set, which is

$$\min_{f(k)} \sum_{i=1}^{N} \frac{\|f(k)\hat{s}_i(k)\|}{\|f(k)\hat{p}(k)\|} \quad \text{subject to} \quad s_i(k) \gg p(k),$$

where k and $f(k)$ are the variable and impulse response of

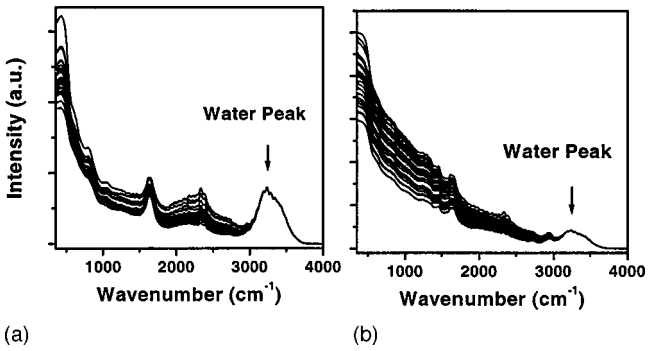

FIG. 3. Calibrated Raman spectra collected from the second group of samples (a) and the third group of samples, the simulated sera (b).

the optimal filter, respectively, $\hat{s}_i(k)=s_i(k)/\|s_i(k)\|$ and $\hat{p}(k)=p(k)/\|p(k)\|$ are the ith normalized spectrum in the calibration set and the normalized pure spectrum, respectively. We used the normalized spectra instead of raw ones to weight equally each spectrum of the calibration set in the procedure of optimization. In the frequency domain, the optimization problem becomes

$$\min_{f(e^{j\omega})} \sum_{i=1}^{N} \frac{\|f(e^{j\omega})\hat{s}_i(e^{j\omega})\|}{\|f(e^{j\omega})\hat{p}(e^{j\omega})\|}.$$

When there is a difference in frequency characteristics between the desired signal and the interfering background, the SBR must have the local maxima at a few certain frequency bands. Therefore, a digital filter can be built to select the frequency bands at which SBR reaches to its maximum. The SBR will be enhanced after processing the raw spectra with the filter. The PLS calibration based on the filtered spectral data should then produce better prediction accuracy. We call this technique the combined multiple bandpass-filtering with PLS method (MFPLS).

IV. RESULTS AND DISCUSSION

The typical Raman spectra of the stock solutions in the second and third groups of the samples are shown in Fig. 3. The spectral range of a full spectrum was from 350 to 4000 cm^{-1} and the spectral acquisition time was 10 s. A five-point adjacent averaging filtering was used to remove the high frequency noise and to preserve the spectral features in the recorded spectral data. All spectra used in the calibration were normalized to the dominant water peak at 3350 cm^{-1}. The fluctuations in the spectra in the range from 350 to 3000 cm^{-1} were partially caused by the thickness variation in the quartz wall of the Raman cells, because the cells were made locally in the university glassblowing facility. The capillary size and wall thickness could not be easily controlled.

We performed PLS calibration and prediction on the spectra collected from the second and third groups of solutions separately. Spectra recorded from 30 samples in each group were used for the calibration. A crossvalidation based on a ''leaving out one spectrum at a time'' procedure was employed to evaluate the average prediction ability for the PLS models built on the calibration set.[23] The prediction accuracy was determined by calculating the root mean

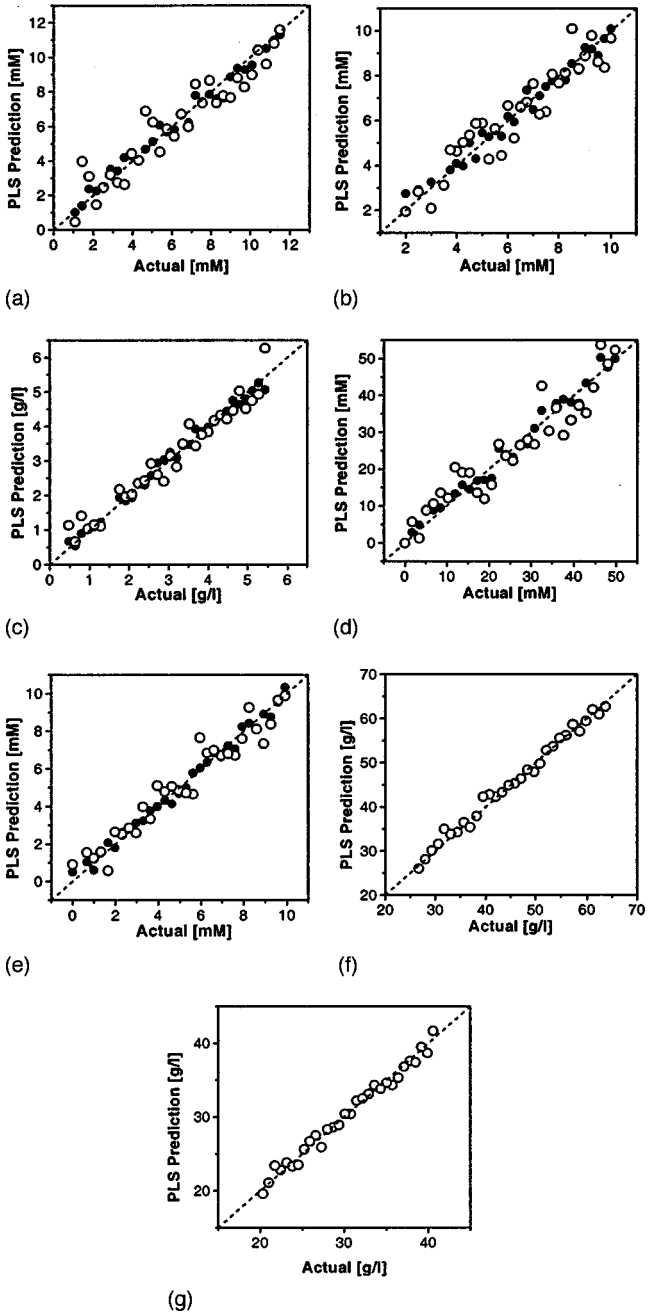

FIG. 4. PLS prediction plots for glucose (a), urea (b), triactin (c), ethanol (d), acetaminophen (e), albumin (f), and globulin (g). The solid circles represent the predicted concentration vs actual concentration in the second group of samples. The open circles represent the predictions in the simulated sera.

squared error of prediction (RMSEP) for the 30 rounds of crossvalidations. Because the albumin and globulin were not added in the second group of samples, the PLS calibration results in the second group of samples should then set the accuracy limits of the Raman tests on glucose, urea, triactin, ethanol, and acetaminophen in mixtures without interference from proteins.

The PLS predicted concentrations of all analytes in two groups of samples versus actual concentrations are shown in Fig. 4. We observe that the errors of prediction for all the analytes obtained in the second group of samples are significantly lower than those in the third group of samples. This

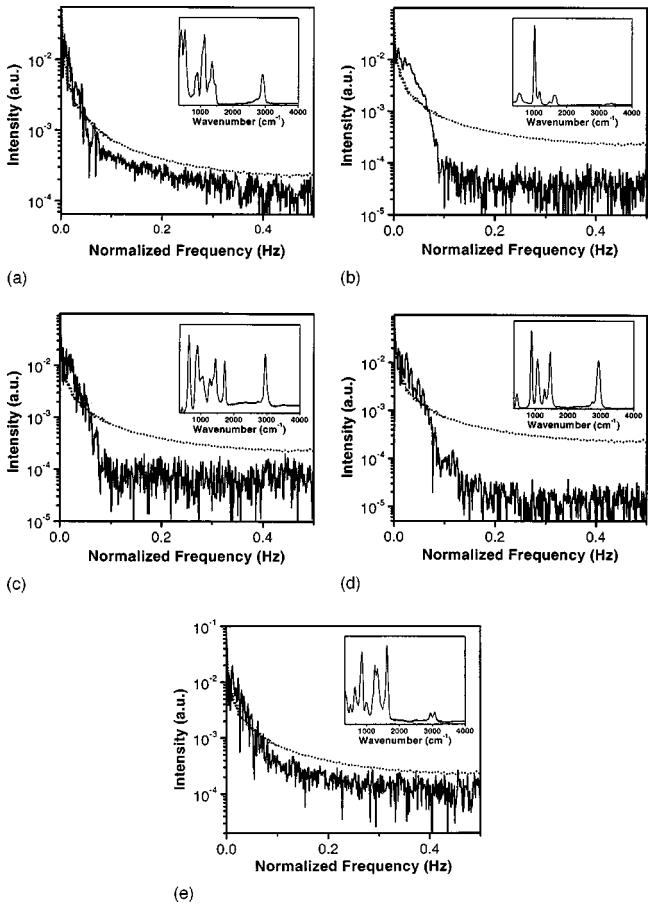

FIG. 5. Pure Raman spectra (insets) and their Fourier transforms of glucose (a), urea (b), triactin (c), ethanol (d), and acetaminophen (e). The Fourier transform of the mean spectrum of the calibration set is presented in dotted lines.

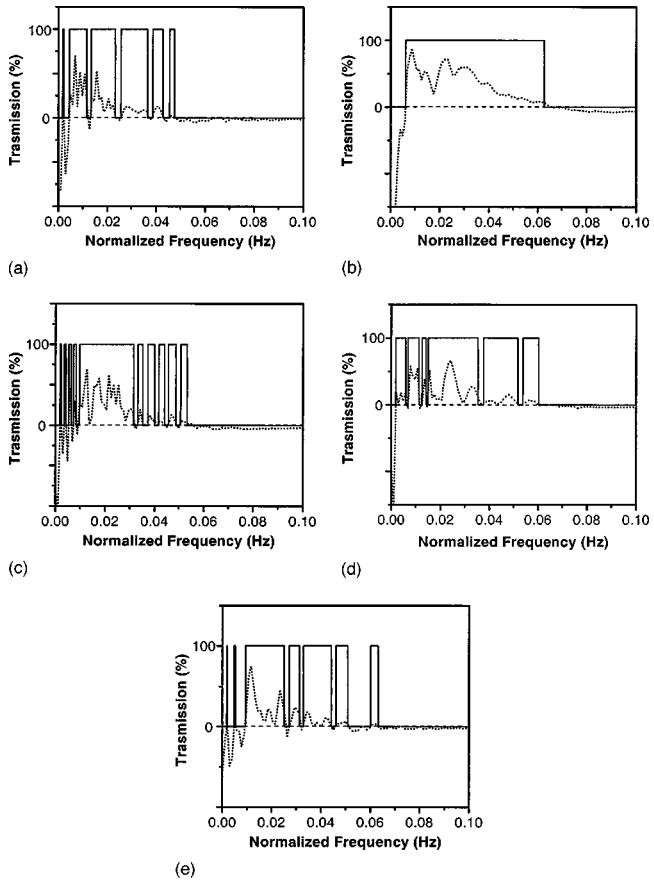

FIG. 6. Optimal wavelength bands for glucose (a), urea (b), triactin (c), ethanol (d), and acetaminophen (e). The differential spectra (dotted lines) are scaled up for better illustration of the high SBR bands and low SBR bands.

demonstrates once again that the presence of proteins confounds the PLS calibration and contributes to the errors of prediction for the analytes with small Raman signals in serum such as glucose, urea, etc. However, the prediction accuracy of albumin and globulin were very high because the Raman signals for proteins are much higher than for other small molecules in the serum.[6,7]

To design a multiple bandpass filter for the enhancement of SBR and improvement of PLS calibration, we studied the Fourier frequency characteristics of the pure spectra and the interfering background. Pure spectra of glucose, urea, triactin, ethanol, and acetaminophen were obtained by subtracting the PBS spectrum from the spectra collected from the first group of stock solutions. To ensure the accurate extraction of the pure spectrum, the same Raman cell was used to measure the spectra of PBS and the five stock solutions. The spectral acquisition time was set to 60 s. Figure 5 shows the pure spectra of glucose, urea, triactin, ethanol, and acetaminophen, and their normalized Fourier frequency spectra. The normalized Fourier transform of the mean spectrum of the calibration set, $\overline{\hat{s}(e^{j\omega})}$, is shown in the same figure as the reference. As can be seen, the distribution of the major frequency components for the pure signals and the background are in the range of normalized frequencies from 0 to 0.15 Hz. Intuitively, the SBR at the frequency bands, where $\hat{p}(e^{j\omega})$ is greater than $\hat{s}(e^{j\omega})$, should be higher than the SBR of the raw signal, and the SBR should be lower than the SBR of the raw signal in the frequency range where $\hat{p}(e^{j\omega})$ is lower than $\hat{s}(e^{j\omega})$. The optimization problem then becomes selecting the frequency components with high SBR and rejecting the components with low SBR.

We used the exhaustive search method to find the optimal frequency bands. The initial bands for the search were defined by the function of $\Gamma(\omega)=\{\mathrm{Sgn}[\hat{p}(e^{j\omega})-\overline{\hat{s}(e^{j\omega})}]+1\}/2$, which selects all the frequency bands making the SBR higher than that of the spectra in the calibration set. The finite impulse response (FIR) filter, a commonly used digital filter with stable performance,[24] was used to form the multiple bandpass filter. One FIR filter was employed in each single frequency band. The Γ function here determined the total number of FIR bandpass filters used. We cut off all the frequency components beyond 0.15 Hz because their contributions to the total signal were negligible. During the optimization, the bandwidth and central frequency of each FIR filter was allowed to change in its corresponding frequency range as long as there was not an overlap between the adjacent FIR filters. The optimal filter was determined when the PLS model based on the filtered calibration set produced the lowest RMSEP during cross-validation.

The optimal frequency bands for glucose, urea, triactin, ethanol, and acetaminophen are shown in Fig. 6. The differ-

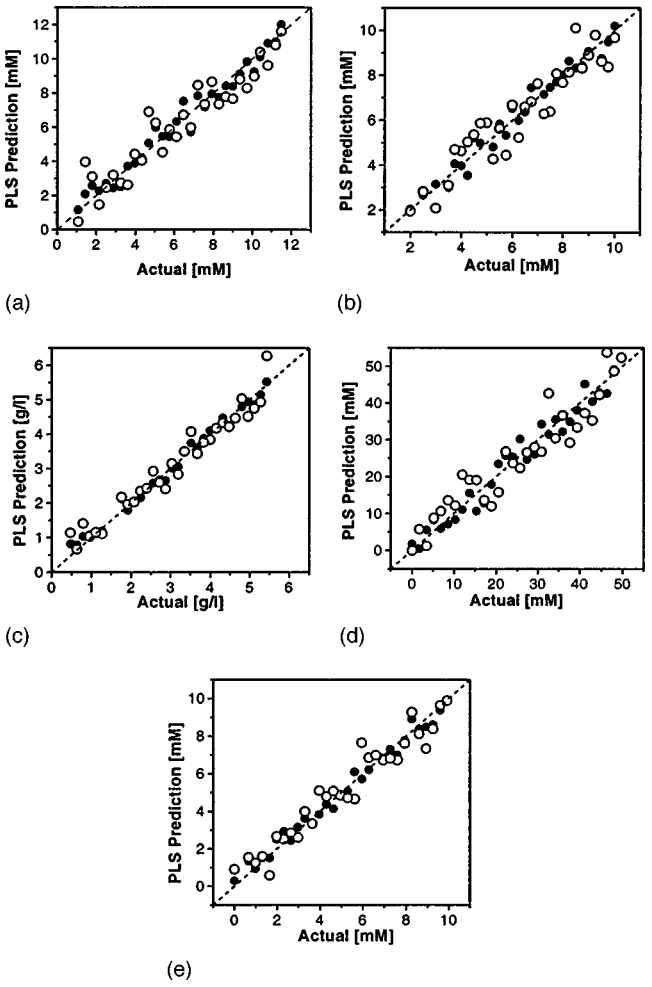

FIG. 7. MFPLS and PLS prediction plots for glucose (a), urea (b), triactin, ethanol (c), and acetaminophen (d). The solid circles represent the MFPLS predictions and the open circles represent the PLS predictions.

ential spectra between the Fourier transforms of the pure spectra and the background are displayed as the references. It is not surprising that the optimal frequency bands are almost the same as those defined by the Γ function. This means that the optimal filter selects most of the frequency components with an SBR higher than the raw data and rejects the components with an SBR lower than the raw data. A comparison between the PLS predictions for the five analytes in the simulated sera based on raw data and filtered data is shown in Fig. 7. We observe that the MFPLS method substantially improves the prediction accuracy for all the analytes. The RMSEP and r^2 values for glucose, urea, triactin, ethanol, and acetaminophen generated by two methods are summarized in Table I. The RMSEP and r^2 values produced by PLS in the second group of samples, the mixtures of the five analytes, are presented as the limits of the prediction accuracy. As can be seen, the RMSEP values in the predictions of all the five analytes obtained by MFPLS method are comparable with those produced by PLS in the mixtures of the five analytes. The results demonstrate that optimal filtering improves PLS calibration while enhancing the SBR and suppressing the confounding of desired signals by proteins, the major interferants.

In conclusion, we developed a near-IR laser Raman instrument equipped with the software of multiple bandpass filtering and PLS calibrations for potentially rapid and reagentless quantification of clinically important analytes in a submicroliter simulated human serum sample. In principle, the serum sample centrifuged from a drop of blood is adequate for the Raman tests in the clinical practice. The Raman signal acquisition can be completed in 10 s. The time for signal processing and PLS prediction is less than a second using a Pentium III computer. The signal self-calibration mechanism makes spectral acquisition insensitive to the variation of excitation/collection optics and excitation power, and makes quantitative Raman tests practical at clinical level. The results demonstrate that with this instrument the prediction accuracy for glucose, urea, triactin, albumin, globulin, ethanol, and acetaminophen is greatly acceptable for clinical diagnosis.[6,7,12,25]

TABLE I. Comparison of RMSEP and r^2 for PLS and MFPLS.

	RMSEP values[a]			r^2 values		
	PLS	MFPLS	Ref.[b]	PLS	MFPLS	Ref.[b]
Glucose	1.0	0.52	0.41	0.90	0.97	0.99
Urea	0.80	0.42	0.35	0.88	0.97	0.98
Triactin	0.34	0.16	0.14	0.95	0.99	0.99
Ethanol	4.9	2.7	2.1	0.89	0.97	0.98
Acetaminophen	0.74	0.36	0.3	0.93	0.99	0.99
Albumin	1.2			0.99		
Globulin	0.8			0.98		

[a]The unit for glucose, urea, ethanol, and acetaminophen is mM and the unit for triactin, albumin, and globulin is g/l.
[b]The RMSEP and r^2 values obtained from the PLS calibration on the spectra measured in the mixtures of glucose, urea, ethanol, and acetaminophen in PBS.

However, it should be pointed out that the Raman signal collection optics used in this study does not take the advantage of the signal enhancement of the waveguide cell.[8,26,27] The major technical obstacles to limit the application of the signal enhancement effect in a practical spectroscopy instrument are that the signal is strongly dependent on the cleanliness of the external cell surface and the active part of the cell must be ''floating'' in the air to ensure that the waveguide condition is satisfied.[26] This causes problems in measurement reproducibility, waveguide handling and optical alignment. Very recently, a liquid waveguide for Raman spectroscopy in aqueous solution was reported. A material called Teflon-AF with a refractive index of 1.29–1.31 was used to make the capillary.[26] The capillary acts as the cladding of the liquid waveguide because its refractive index is smaller than that of water. The excitation light and guided Raman signal do not reach to the surface of the capillary. The problems with conventional waveguide cells are thus overcome. Moreover, the Raman signal from the cell material is weak and negligible.[26] This eliminates the possible interference from the cell material. In a future study, we will use the capillary made with the material of a refractive index lower than water as the Raman cell and use the coaxial excitation/collection geometry to take the advantage of signal enhancement.[8,26,27] The performance of the Raman instrument used in this study is therefore expected to be further improved. It also should be noted that though the samples

used in this work consisted of the major biological analytes in human sera, the chemical profile of a real serum sample is more complicated. For instance, the procedure to extract the serum from the fresh blood may produce little hemoglobin caused by the breakdown of red cells, which may create interference for the Raman tests. Further investigations are needed to confirm if the same prediction accuracy in simulated sera can be achieved in real human sera.

ACKNOWLEDGMENT

This work was supported by Hong Kong Research Council Grant No. HKUST6207/98P.

[1] C. G. Kontoyannis and M. Orkoula, Talanta **41**, 1981 (1994).
[2] M. J. Goetz, Jr., G. L. Cote, R. Erckens, W. March, and M. Motamedi, IEEE Trans. Biomed. Eng. **42**, 728 (1995).
[3] J. P. Wicksted, R. J. Erckens, M. Motamedi, and W. F. March, Appl. Spectrosc. **49**, 987 (1995).
[4] J. Berger, Y. Wang, and M. S. Feld, Appl. Opt. **35**, 209 (1996).
[5] X. Dou, Y. Yamaguchi, H. Yamamoto, S. Doi, and Y. Ozaki, Vib. Spectrosc. **13**, 83 (1996).
[6] A. J. Berger, T. W. Koo, I. Itzkan, G. Horowitz, and M. S. Feld, Appl. Opt. **38**, 2916 (1999).
[7] J. N. Y. Qu, B. C. Wilson, and D. Suria, Appl. Opt. **38**, 5491 (1999).
[8] G. E. Walfrafen and J. Stone, Appl. Spectrosc. **26**, 585 (1972).
[9] K. Fujiwara, S. Ito, R. E. Kojyo, H. Tsubota, and R. L. Carter, Appl. Spectrosc. **46**, 1032 (1992).
[10] M. J. Mattu, G. W. Small, and M. A. Arnold, Anal. Chem. **69**, 4695 (1997).
[11] C. Lentner, *Geig Scientific Tables* (Ciba-Geigy, New Jersey, 1981), Vol. 3, pp. 89–115.
[12] N. W. Tietz, *Clinical Guide to Laboratory Tests* (Saunders, Philadelphia, 1995), pp. 787–897.
[13] B. K. Lavine, Anal. Chem. **72**, 91R (2000).
[14] D. M. Haaland and E. V. Thomas, Anal. Chem. **60**, 1193 (1988).
[15] H. Martens and T. Naes, *Multivariate Calibration* (Wiley, New York, 1989).
[16] R. E. Shaffer, G. W. Small, and M. A. Arnold, Anal. Chem. **68**, 2663 (1996).
[17] D. Jouan-Rimbaud, B. Walczak, R. J. Poppi, O. D. Noord, and D. L. Massart, Anal. Chem. **69**, 4317 (1997).
[18] J. H. Kalivas, N. Roberts, and J. M. Sutter, Anal. Chem. **61**, 2024 (1989).
[19] A. S. Bangalore, R. E. Shaffer, G. W. Small, and M. A. Arnold, Anal. Chem. **68**, 4200 (1996).
[20] M. J. McShane, B. D. Cameron, G. L. Cote, M. Motamedi, and C. H. Spielgeman, Anal. Chim. Acta **388**, 251 (1999).
[21] C. H. Spiegelman, M. J. McShane, M. J. Goetz, M. Motamedi, Q. L. Yue, and G. L. Cote, Anal. Chem. **70**, 35 (1998).
[22] A. J. Berger, T. W. Koo, I. Itzkan, and M. S. Feld, Anal. Chem. **70**, 623 (1998).
[23] R. G. Brereton, *Chemometrics: Applications of Mathematics and Statistics to Laboratory Systems* (Ellis Horwood, New York, 1990), pp. 219–221.
[24] N. J. Loy, *An Engineer's Guide to FIR Digital Filters* (Prentice-Hall, Englewood Cliffs, NJ, 1988).
[25] The U. S. Department of Health and Human Services: Clinical Laboratory Improvement Amendments of 1988; Final Rules and Notice, 42 CFR Part 493. The Federal Register, **57**, 7188 (1992).
[26] L. Song, S. Y. Liu, V. Zhelyaskov, and M. A. Elsayed, Appl. Spectrosc. **52**, 1364 (1998).
[27] Z. Y. Zhu and M. C. Yapert, Anal. Chem. **66**, 761 (1994).